Kidney International, Vol. 68 (2005), pp. 1543–1553

Crystals cause acute necrotic cell death in renal proximal tubule cells, but not in collecting tubule cells

MARIEKE S.J. SCHEPERS, EDDY S. VAN BALLEGOOIJEN, CHRIS H. BANGMA, and CARL F. VERKOELEN

Department of Urology, Erasmus Medical Center, Rotterdam, The Netherlands

Crystals cause acute necrotic cell death in renal proximal tubule cells, but not in collecting tubule cells.

Background. The interaction between renal tubular cells and crystals generated in the tubular fluid could play an initiating role in the pathophysiology of calcium oxalate nephrolithiasis. Crystals are expected to form in the renal collecting ducts, but not in the proximal tubule. In the present investigation, we studied the damaging effect of calcium oxalate crystals on renal proximal and collecting tubule cells in culture.

Methods. Studies were performed with the renal proximal tubular cell lines, porcine proximal tubular cells (LLC-PK_1) and Madin-Darby canine kidney II (MDCK-II) and the renal collecting duct cell lines, $RCCD_1$ and MDCK-I. Confluent monolayers cultured on permeable growth substrates in a two-compartment culture system were apically exposed to calcium oxalate monohydrate crystals, after which several cellular responses were studied, including monolayer morphology (confocal microscopy), transepithelial electrical resistances (TER), prostaglandin E_2 (PGE_2) secretion, DNA synthesis ([^{3}H]-thymidine), total cell numbers, reactive oxygen species [hydrogen peroxide (H_2O_2)] generation, apoptotic (annexin V and DNA fragmentation), and necrotic (propidium iodide influx) cell death.

Results. Crystals were rapidly taken up by proximal tubular cells and induced a biphasic response. Within 24 hours approximately half of the cell-associated crystals were released back into the apical fluid (early response). Over the next 2 weeks half of the remaining internalized crystals were eliminated (late response). The early response was characterized by morphologic disorder, increased synthesis of PGE_2, H_2O_2, and DNA and the release of crystal-containing cells from the monolayers. These released cells appeared to be necrotic, but not apoptotic cells. Scrape-injured monolayers generated even higher levels of H_2O_2 than those generated in response to crystals. During the late response, crystals were gradually removed from the monolayers without inflammation-mediated cell death. Crystals did not bind to, were not taken up by, and did not cause marked responses in collecting tubule cells.

Conclusion. This study shows that calcium oxalate crystals cause acute inflammation-mediated necrotic cell death in renal proximal tubular cells, but not in collecting tubule cells. The crystal-induced generation of reactive oxygen species by renal tubular cells is a general response to tissue damage and the increased levels of DNA synthesis seem to reflect regeneration rather than growth stimulation. As long as the renal collecting ducts are not obstructed with crystals, these results do not support an important role for crystal-induced tissue injury in the pathophysiology of calcium oxalate nephrolithiasis.

Key words: calcium oxalate crystals, inflammation, necrotic cell death, renal proximal and collecting tubule cells.

Received for publication October 26, 2004
and in revised form January 6, 2005, and March 9, 2005
Accepted for publication May 5, 2005

Kidney stones are composed of numerous microcrystals accumulated in the kidney. The human kidney produces concentrated urine commonly supersaturated with poorly soluble salts like calcium oxalate. The precipitation of these salts as crystals is common and harmless as long as these crystals are excreted with the urine. To ensure their efficient elimination, the renal epithelial lining should be nonadherent in nephron segments with high levels of supersaturation. Compared to nonstone formers, the levels of stone salt supersaturation are usually higher in urine of recurrent stone formers, which is why these patients often excrete higher amounts of crystals. Crystal binding to renal tubular cells may be the underlying cause of nephrocalcinosis and nephrolithiasis. Perhaps there are pathologic circumstances during which healthy cells are transformed in a crystal binding phenotype.

The impression that the crystals themselves could be actively involved in this process came from studies performed in animals and in cell culture [1–4]. These studies suggested that calcium oxalate crystals generate free radicals that are damaging to the renal tubular cells. There are some questions, however, about the model systems used. In animals, calcium oxalate crystalluria cannot exist without hyperoxaluria which makes it difficult to discriminate between effects caused by crystals or by oxalate. Another point of concern is that most calcium oxalate toxicity studies are performed with renal proximal tubular cells while crystal formation is extremely unlikely in this nephron segment.

In the present investigation, we studied the possible toxic effect of calcium oxalate crystals to renal proximal and collecting tubule cells grown as confluent monolayers on permeable growth substrates in a two-compartment

culture system. In this model system, the apical compartment is representative for the tubular fluid, whereas the basal compartment is representative for the interstitial space and blood supply. Crystals are added at the luminal side of the monolayers in serum-free growth medium, while serum-containing growth medium is added to the basal compartment. Thus, during their apical exposure to calcium oxalate crystals, the cells have free access to serum components from the basolateral membrane. The results show that under these conditions calcium oxalate crystals are toxic to renal proximal tubular cells, but not to collecting duct cells.

METHODS

Cell culture

Madin-Darby canine kidney (MDCK)-I and MDCK-II cells were kindly provided by Professor G. van Meer (Laboratory for Cell Biology and Histology, Amsterdam Medical Center, The Netherlands) [5]. Porcine proximal tubular cells (LLC-PK_1) were obtained from the American Type Culture Collection (ATCC) (Manassas, VA, USA). Rat renal cortical collecting duct ($RCCD_1$) cells [6] were kindly provided by Dr. M. Blot-Chabaud (INSERM U246, Faculté de Médecine Xavier Bichat, Paris, France). Routinely, cells were grown in Dulbecco's modified Eagle's medium (DMEM) (Gibco, Grand Island, NY, USA), supplemented with 10% fetal calf serum (FCS) (PAA Labs, Linz, Austria), and weekly replated. Cells were cultured at intermediate densities in polystyrene tissue culture treated 75 cm^2 flasks (Falcon) (BD Biosciences, Bedford, MA, USA) and the culture medium refreshed twice a week. For experiments cells were trypsinized and seeded at a concentration of 1 ± 10^6 cells/polycarbonate permeable support (Transwells) (24 mm diameter inserts, 4.7 cm^2 surface area, 0.4 μm pore size) (Corning Costar, Badhoevedorp, The Netherlands). Within 6 to 7 days the cells proliferated and migrated into confluent monolayers with, depending on the cell type, a cell density of 4 to 6 ± 10^6 cells.

To study crystal-cell interaction, confluent monolayers were washed after which serum-free DMEM (1.5 mL) was added to the apical compartment, whereas the basal compartment received DMEM 10% FCS (2.6 mL) and 100 μL (146 μg) calcium oxalate monohydrate crystal suspension was added at the apical side of the monolayers.

Tight junction formation is assessed by transepithelial electrical resistance (TER) measurements. TER is measured in ohms (Ω) after placing the insert in an Endohm 24 connected to a Voltohm meter (World Precision Instruments, Sarasota, FL, USA). Monolayers are considered confluent as soon as the highest TERs are reached. Routinely, polymerase chain reaction (PCR) analyses were performed on DNA isolated from cell culture conditioned medium for the presence of mycoplasma. Cells used in this study were not contaminated with mycoplasma.

Crystal formation in cell culture medium

To reveal at which concentrations oxalate induces crystal formation in culture medium, increasing amounts of oxalate were added to DMEM containing 1.8 mmol/L calcium. Sodium oxalate was dissolved in Milli-Q distilled water and added at the appropriate concentration in a small volume on the bottom of a tube. Subsequently 50 mL DMEM was added at room temperature and the tube immediately vigorously shaken. After centrifugation at low speed (1000 rpm), the pellet was inspected by phase-contrast microscopy. Another approach was applied to study crystal formation at different temperature and in the presence or absence of FCS. A tracer amount of [^{14}C]-oxalate was mixed with unlabeled oxalate and added to 10 mL DMEM of 20°C and 37°C with and without 5% FCS to give a final oxalate concentrations of 0, 0.5, 1.0, and 2 mmol/L. The tubes were centrifuged, washed one time with calcium oxalate–saturated water, centrifuged again, and the pellet dissolved in 1 mL 1 mol/L perchloric acid. This solution was transferred to a vial with 10 mL scintillation fluid and counted in a scintillation counter (Packard, Meriden, CT, USA). The solid radioactivity in the tubes was expressed as dpm/pellet.

Morphologic studies

Several staining procedures were used to visualize aspects of crystal-induced cell responses by confocal microscopy. To monitor cell-associated crystals light reflection was applied to visualize the localization of the crystals and fluorescein isothiocyanate (FITC)-conjugated phalloidin to stain polymeric F actin in the cell cytoskeleton. At the various time points, filter inserts were washed three times with physiologic saline [phosphate-buffered saline (PBS)] and fixed for 15 minutes in ethanol 70%. Previously, it was demonstrated that fixation with ethanol releases most of the crystals that are loosely associated with the cell surface [7]. Ethanol-fixed cells are subsequently incubated for 15 minutes with 5 μg/mL phalloidin-FITC (Sigma Aldrich Chemie BV, Zwijndrecht, The Netherlands), washed three times and mounted in Vectashield (Vector Laboratories, Burlingame, CA, USA). To study the subcellular localization of crystals under the various conditions, XY scans in a focal plane (horizontal) and cross-sectional XZ scans (vertical) were made with a Zeiss LSM 510 Meta (Zeiss, Oberkochen, Germany) [8]. A 488 nm argon laser was used to excite the FITC phalloidin. Crystals was detected by 633 nm (red) Krypton laser light reflection. A 560 nm beam splitter separated the FITC emission signal and the 633 nm signal reflected by the crystals. The FITC signal was passed through a 510 to 540 nm band-pass filter

to block the reflection from the 488 nm laser. No blocking filter was used for the light reflection signal. The mounted inserts were extensively inspected and images (magnification 63±) were made of at least 10 random fields per insert from which representative images were selected. Experiments were repeated at least three times.

Calcium oxalate monohydrate crystal binding

A solution of radiolabeled sodium oxalate was prepared by adding 10 μL 37 MBq/mL [^{14}C]-oxalic acid (Amersham Int. plc, Buckinghamshire, UK) to 0.25 mL 200 mmol/L sodium oxalate. A calcium chloride solution was prepared by adding 0.25 mL 200 mmol/L $CaCl_2$ to 9.5 mL distilled water. Mixing the two solutions at room temperature (final concentration of 5 mmol/L for both oxalate and calcium) immediately resulted in the nucleation of radiolabeled calcium oxalate monohydrate. After settling for 3 days, crystals were washed three times with and resuspended in calcium oxalate–saturated H_2O in a final volume of 5 mL (1.46 mg calcium oxlate monohydrate crystals/mL). In this study the cells were incubated with 100 μL crystal suspension (146 μg/insert or 32 μg/cm^2). The same procedure but without [^{14}C]-oxalic acid was used for the generation of nonradiolabeled calcium oxalate monohydrate. The crystals prepared with this method consist entirely of calcium oxalate monohydrate with an average size of 1 to 2 μm [9].

To quantify the amount of calcium oxalate monohydrate crystals that remained associated with the monolayers in time, radiolabeled crystals were added at the luminal side of confluent monolayers in serum-free DMEM, while in the basal compartment the cells received DMEM 0.5% FCS. Cells were incubated for 1 hour, after which the inserts were rinsed to remove all nonassociated crystals, cut out, and placed in a scintillation vial. To extract radioactivity, 1 mL 1 mol/L perchloric acid was added and the amount of radioactivity was counted in a liquid scintillation counter (Packard). The amount of associated crystals was calculated from the dpm/filter. The remaining inserts were extensively washed after which the apical compartment received serum-free DMEM, whereas DMEM 10% FCS was added to the basal compartment. The procedure to assess the amount of cell-associated radioactivity was subsequently repeated 1, 2, 7, and 15 days postincubation.

To study the ability of the cells to process internalized crystals the following study was conducted. Monolayers were incubated for one hour with [^{14}C]-calcium oxalate monohydrate according the method described above. Twenty-four hours postincubation, released or loosely attached crystals were removed through extensive washing of the monolayers. During the days thereafter and starting 2 days postincubation, the fluid in the apical and basal compartments was collected and centrifuged. The amount of radioactivity was counted in 100 μL portions in the supernatants and in the pellets after dissolution in 1 mol/L perchloric acid. The amount of [^{14}C]-calcium oxalate monohydrate that remained associated with the monolayers was counted in a scintillation counter.

Hydrogen peroxide (H_2O_2)

The reactive oxygen intermediate H_2O_2 was measured in the apical fluid of cells exposed to various concentrations of crystals using the Amplex Red Hydrogen/Peroxide Assay Kit (A-22188) (Molecular Probes, Leiden, The Netherlands). Since phenol red in the culture medium interferes with the absorbance measurements the studies are performed with a buffer containing (in mmol/L): 124 NaCl, 25 $NaHCO_3$, 2 $NaH_2PO_4.2H_2O$, 5 KCl, 0.5 $MgCl_2.6H_2O$, 5 Na-acetate, pH 7.4, 310 to 320 mOsmol/kg H_2O (calcium-free buffer B), added to the apical fluid compartment, while the basal compartment received DMEM 10% FCS without phenol red and sodium pyruvate (Gibco). A standard curve was prepared at 10 μmol/L to 1.25 μmol/L. Samples, standards, and blank were aliquoted to a 96-well plate. A working solution of 100 μmol/L Amplex red reagent and 0.2 U/mL horseradish peroxidase was prepared and added to all the samples, standards, and blank. The plate was protected from light and incubated for 30 minutes at room temperature. The absorbance was read at 560 nm using a Bio-Rad 550 microplate reader (Bio-Rad, Hercules, CA, USA).

Prostaglandin E_2 (PGE_2)

PGE_2 secreted into the luminal compartment was measured in a switch enzyme-linked immunoassay (EIA) Kit (Cayman, Ann Arbor, MI, USA). This assay is based on the competition between PGE_2 and a PGE_2-acetylcholinestrase (AchE) conjugate (as tracer) for a limited amount of PGE_2 monoclonal antibody. Because the concentration of the PGE_2 tracer is held constant while the concentration of PGE_2 varies, the amount of PGE_2 tracer that is able to bind to the PGE_2 antibody was inversely proportional to the concentration of PGE_2 in the well. PGE_2 standard curves were prepared by diluting 10 mg/mL PGE_2 in EIA buffer to produce a concentration range of 0 to 1000 μg PGE_2/mL. Each plate or set of strips contained a blank, a nonspecific binding, a maximum binding, and a total activity control. Standard curve samples (50 μL), controls and experimental samples were added to the wells. Each well received 50 μL tracer except the total activity and the blank wells. The wells subsequently received 50 μL PGE_2 monoclonal antibody except the total activity well, the nonspecific binding well, and the blank well. The plate was covered with plastic film and incubated for 18 hours at 4°C. The wells

were rinsed extensively with wash buffer after which 200 μL Ellman's Reagent was added to each well and 5 μL tracer to the total activity well. The plate was then covered with plastic film and developed in the dark on an orbital shaker. When the blank absorbance was between 0.3 and 0.8 units, the plate was read in a Bio-Rad model 550 microplate reader at 405 to 420 nm wavelengths.

[^{3}H]-thymidine incorporation

To assess the effect of crystals on DNA synthesis, monolayers were incubated for 24 hours with 146 μg calcium oxalate monohydrate after which all nonassociated crystals were removed by extensive washing and the monolayers received fresh DMEM 10% FCS containing 3.7 KBq/mL [methyl-^{3}H]-thymidine (Amersham Biosciences). After a pulse labeling period of 3 hours, the cultures were washed three times with PBS, the filters cut out, and counted in a liquid scintillation counter. Results are expressed in dpm/filter insert.

Crystal-induced apoptotic or necrotic cell death

To assess the nature of crystal-induced cell death, annexin V (A.G. Scientific, Inc., San Diego, CA, USA) staining was applied to reveal the surface exposure of phosphatidylserine (apoptosis) and propidium iodide (Sigma Aldrich Chemie) to reveal the loss of plasma membrane integrity (necrosis). At the various time points, filter inserts were washed and unfixed cells were incubated for 15 minutes with FITC-labeled annexin V (1:40), washed three times, and subsequently incubated for 15 minutes with 1 μg/mL propidium iodide, washed, and mounted in Vectashield (Vector Laboratories). Another widely applied method to study apoptosis is DNA fragmentation staining with Hoechst 33258 (Sigma Aldrich Chemie). At the various time points, filter inserts were washed and incubated with 0.1 mg/mL Hoechst, washed, and mounted in Vectashield. In some experiments propidium iodide influx or Hoechst in combination with light reflection (crystals) was applied to assess if crystal-cell interaction is accompanied with apoptotic or necrotic cell death. Incubation of the cells for 4 hours with 1.0 μmol/L antimycin A (Sigma Aldrich, Zwijndrecht, The Netherlands) was used as positive control for apoptosis, while cell fixation with ethanol to permeabilize the membrane served as positive control for necrosis. Phase-contrast microscopy was applied to monitor the release of crystal-containing cells in the apical fluid compartment.

Statistics

Student *t* tests and analysis of variance (ANOVA) were performed using triplicate samples and repeated at least two times to assess the statistical significance between data points. Differences were considered statistically significant at $P < 0.05$.

RESULTS

Oxalate-induced crystal formation in culture medium

One of the motives to study the cellular response to calcium oxalate crystals was that oxalate is often added to calcium-containing culture media without sufficiently taken into account the risk for crystal formation. Effects attributed to oxalate in these studies can be partially or entirely be caused by crystals. In Figure 1A we show the oxalate concentrations inducing calcium oxalate crystal formation in DMEM (1.8 mmol/L calcium). Calcium oxalate crystals were formed after the addition of ≥0.5 mmol/L sodium oxalate (Fig. 1).

This study was repeated with [^{14}C]-oxalate that confirmed that solid radiolabeled material was formed progressively after the addition of ≥0.5 mmol/L oxalate to 20°C or 37°C DMEM containing 0 or 5% FCS (Fig. 1B).

Morphologic studies

Confluent monolayers were incubated for various periods of time with calcium oxalate monohydrate crystals and studied by confocal laser scanning microscopy (CLSM) to monitor crystal localization and to reveal possible crystal-induced alterations in cell shape or behavior compared to cells of the same age that did not receive crystals. XY images of phalloidin FITC-stained cells in combination with light reflection demonstrated no particles in cells that did not receive crystals (Fig. 2A) and crystals inside MDCK-II, 1 day (Fig. 2B) and 7 days (Fig. 2C) after a 1-hour incubation with 146 μg calcium oxalate monohydrate, which was also observed in LLC-PK$_1$ cells (not shown). As reported previously, crystals did not bind to and were not internalized by MDCK-I or RCCD$_1$ cells [7]. After 24 hours, the morphologic appearance of crystal-containing cells was rather disorderly and images made perpendicular to the growth substrate (XZ images) revealed the release of crystal-containing cells into the apical fluid (Fig. 2D). Exfoliation of cells with crystals was confirmed by phase-contrast microscopy showing birefringent crystals in and around released single cells (Fig. 2E). After this initial vigorous response, the cells in the monolayers seemed to accept internalized crystals. After 7 days the quiescent and functional monolayers still contained cells with internalized crystals (Fig. 2C).

Calcium oxalate monohydrate crystal binding

Since it is not possible from CLSM images to appreciate quantitative variations, this study was repeated with radiolabeled crystals. Confluent monolayers of MDCK-II cells were incubated for 1 hour with 146 μg [^{14}C]-calcium oxalate monohydrate. After extensive washing to remove

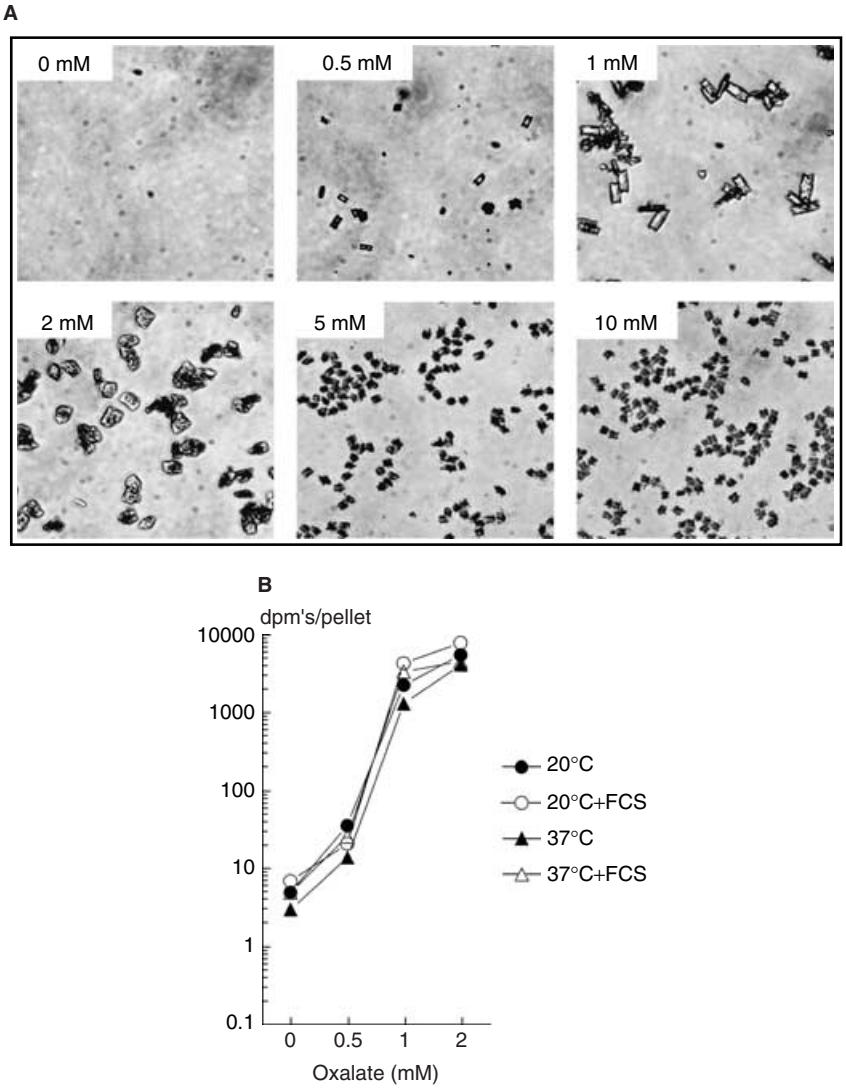

Fig. 1. Calcium oxalate crystal formation after adding sodium oxalate to Dulbecco's modified Eagle's medium (DMEM). (*A*) Crystals are detected by phase-contrast microscopy at oxalate concentrations ≥0.5 mmol/L added to 1.8 mmol/L calcium-containing growth medium. (*B*) Radiolabeled crystals are formed immediately and progressively after the addition of 0, 0.5, 1, and 2 mmol/L [^{14}C]-oxalate to 10 mL 20°C and 37°C DMEM with or without 5% fetal calf serum (FCS). Radioactively labeled material centrifuged in a pellet was considered calcium oxalate crystals. This crystalline material was dissolved in 1 mL 1 mol/L percloric acid and counted in a scintillation counter. The process of crystal formation was hardly affected by the two temperatures used or by the presence of serum proteins.

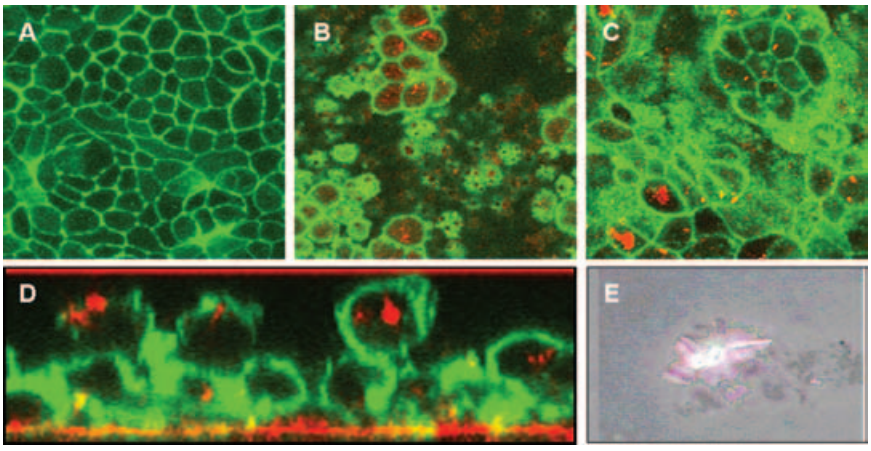

Fig. 2. Confocal laser scanning microscopy images of Madin-Darby canine kidney (MDCK-II) cells cultured on permeable supports in a two-compartment culture system. Cells (green) are visualized with fluorescein isothiocyanate (FITC)-conjugated phalloidin and crystals (red) using light reflection (*A*). Confluent MDCK-II cells incubated for one hour with 146 μg COM crystals. Internalized crystals are found inside cells after 1 (*B*) and 7 days (*C*). An image made perpendicular to the growth substrate 24 hours postincubation revealed that crystal-containing cells were exfoliated from the cultures (*D*), which was confirmed by the presence of crystal-containing cells in the supernatant by phase-contrast microscopy (*E*).

crystals that were not bound to the cells, the amount of monolayer-associated radioactivity was quantified immediately (t = 1 hour) and 1, 2, 7 and 15 days later (Fig. 3). After 1 hour a relatively large amount of crystals were associated with the monolayers. After the first 24 hours, the amount of monolayer-associated radioactivity was reduced by approximately 50% ($T_d \sim 21$ hours) to further decline at a much slower rate in the next 14 days ($T_d \sim 312$ hours). As mentioned above, crystals were eliminated during the initial response by the release of

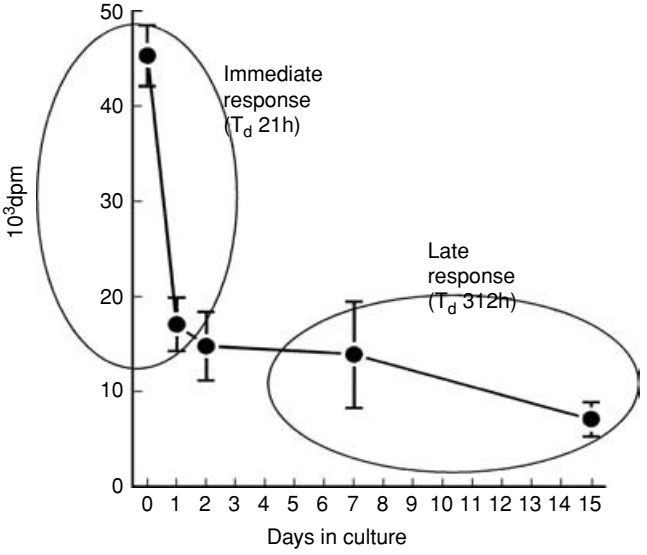

Fig. 3. The elimination of [^{14}C]-calcium oxalate monohydrate by Madin-Darby canine kidney (MDCK)-II cells showed a biphasic pattern. Within the first 24 hours, approximately half of the amount of the crystals that initially became associated with the cells was removed (early response with $T_{d=}$ 21 hours). The cells required another 2 weeks to eliminate again 50% (late response with T_d = 312 hours). The early response may deal with crystals in the plasma membrane, while the late response may deal with internalized crystals.

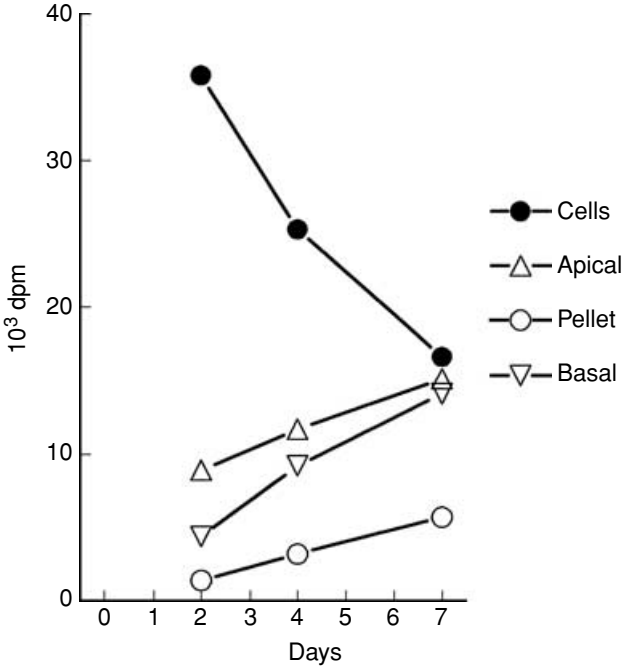

Fig. 4. The elimination of internalized [^{14}C]-calcium oxalate monohydrate during the late response. The crystals are gradually removed from the cultures (•). Approximately 20% was retrieved in the luminal compartment as insoluble material (○). About 80% was recovered as ions that were equally distributed over both the apical (△) and basal (▽) fluid compartment. Because the medium in both fluid compartments was not saturated with calcium oxalate, it is not entirely clear if crystals are dissolved inside cells or in the growth medium.

crystal-containing cells from the monolayers, but we do not exclude the possibility that part of the crystals were translocated back into the apical fluid or rapidly dissolved intracellularly.

To study the cellular handling of endocytosed crystals during the late response, MDCK-II cells were incubated for 1 hour with [^{14}C]-calcium oxalate monohydrate crystals. After extensive washing at 24 hours, the cells were monitored for an additional period of time. Two, 4, and 7 days later, the apical and basal fluid was collected, centrifuged, the filter inserts cut out and radioactivity counted in the pellets, supernatants, and in the cells. Of the total amount of radioactivity eliminated by the monolayer in 5 days ($\sim 20 \pm 10^3$ dpm), approximately 20% (4.3 ± 10^3 dpm) was recovered in the apical fluid as solid material, ~30% (6.2 ± 10^3 dpm) as ion in the apical fluid, and ~50% (9.8 ± 10^3 dpm) as ion in the basal fluid**.** The basolateral fluid did not contain centrifugable material. Since the volume ratio in the apical (1500 μL) and basal (2600 μL) compartment also is approximately 3:5, this suggests that the ion concentration on both sides of the monolayer equilibrated through passive paracellular diffusion. Although about 80% of the eliminated crystals are recovered as ions in the apical and basal fluid compartment this does not necessarily imply that the cells were able to dissolve them. Because the fluid in both compartments was not saturated with calcium and oxalate it is also possible that eliminated crystals dissolved in the growth medium (Fig. 4).

PGE_2

The secretion of PGE_2 into the luminal compartment was measured as marker for crystal-induced inflammation. $RCCD_1$ and $LLC\text{-}PK_1$ appeared to be less suitable for these studies because they produced no or hardly detectable levels of PGE_2. Arachidonic acid is converted to eicosanoids like PGE_2 by cyclooxygenases (COX) and it is known that certain cell lines, including LLC-PK1, have defects in COX activity [10]. These studies were therefore primarily performed with the two MDCK strains. Earlier we found that MDCK cells indeed express COX-2 mRNA (unpublished results). After seeding cells at high densities, both cell types secreted relatively high levels of PGE_2, which steeply decreased after the cultures became confluent (not shown). The exposure of confluent MDCK-II monolayers for 24 hours to calcium oxalate monohydrate induced levels of PGE_2 secretion that were about five times higher than those secreted by control cultures. Although 24 hours' calcium oxalate monohydrate exposure increased the secretion of PGE_2 by MDCK-I cells about twofold, this increase was not statistically significant due to the relatively large standard errors (Fig. 5).

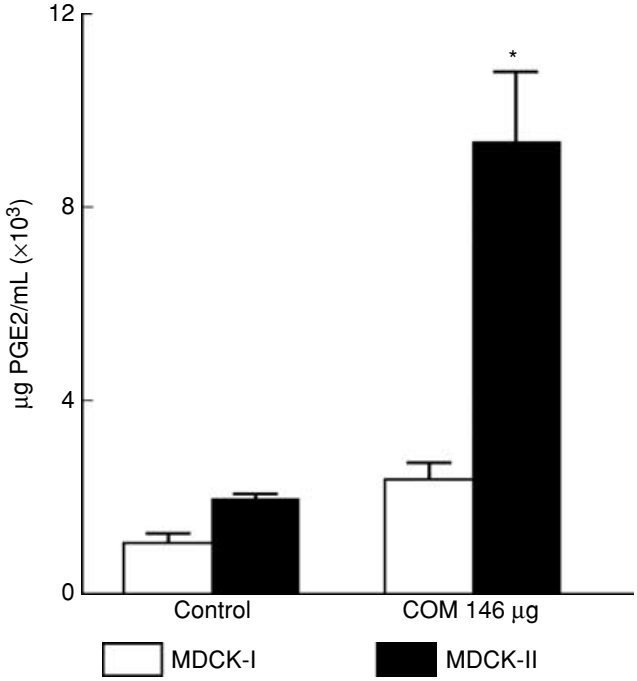

Fig. 5. Prostaglandin E_2 (PGE_2) secretion in response to calcium oxalate monohydrate (COM). The addition of calcium oxalate monohydrate crystals to confluent monolayers increased PGE_2 secretion in Madin-Darby canine kidney (MDCK)-II, but not in MDCK-I. Means ± SD of a representative experiment are shown. Statistical analysis was performed using Student *t* test ($P < 0.05$) ($N = 3$). *Significantly different compared to control.

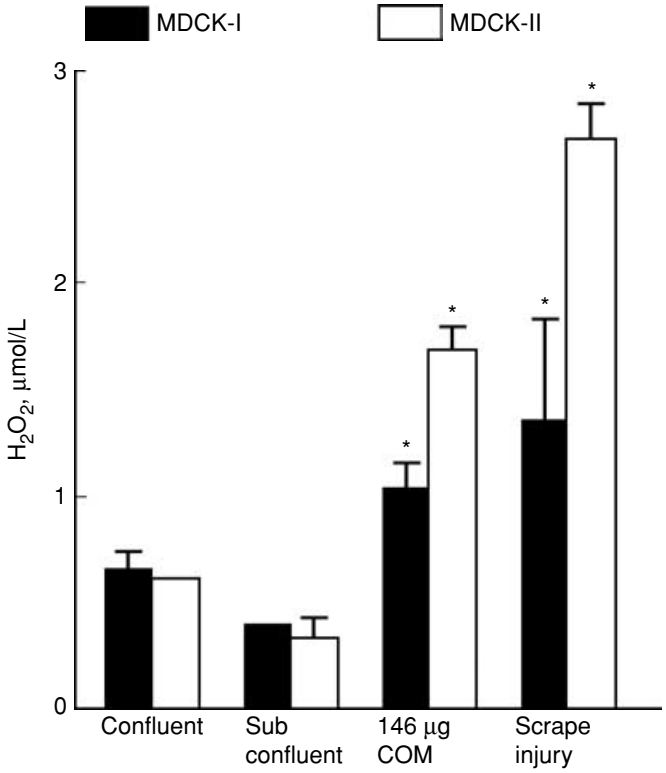

Fig. 6. Confluent monolayers are incubated with 146 µg calcium oxalate monohydrate (COM) crystals or scrape-damaged with the tip of a sterile culture pipette. One day after the addition of crystals or after mechanical damage, H_2O_2 is measured in the apical fluid compartment. The 24-hour conditioned medium of subconfluent and confluent cultures served as controls. Means ± SD of a representative experiment. Statistical analysis was performed using Student *t* test ($P < 0.05$) ($N = 3$). *Significantly different compared to control.

H_2O_2

The production of reactive oxygen species has been proposed as one of the mechanisms by which oxalate and calcium oxalate crystals exert their damaging effect. The production of the reactive oxygen intermediate H_2O_2 was measured in the apical fluid of subconfluent cultures, confluent control cultures, confluent cultures exposed for 24 hours to 146 µg calcium oxalate monohydrate and mechanically damaged confluent monolayers. Compared to confluent cultures, H_2O_2 secretion was not higher in subconfluent cultures, indicating that the generation of reactive oxygen species is not a physiologic event of growth-activated cells. Although the response was larger in MDCK-II, exposure to calcium oxalate monohydrate crystals resulted in increased levels of H_2O_2 production in both MDCK cell lines, as well as in scrape-injured monolayers (Fig. 6).

[^{3}H]-thymidine incorporation

To study the effect of crystals on DNA synthesis, cells with and without crystals were pulse-labeled (3 hours) with [^{3}H]-thymidine, directly or 1 day after a 24-hour incubation with 146 µg calcium oxalate monohydrate. [^{3}H]-thymidine incorporation was significantly higher 2 days after incubating MDCK-II with calcium oxalate monohydrate crystals, while calcium oxalate monohydrate did not affect MDCK-I proliferation (Table 1). Considering the release of MDCK-II cells from the monolayer (24 hours post-calcium oxalate monohydrate) and the time required for DNA synthesis to become significantly increased (48 hours post-calcium oxalate monohydrate), these results suggest that the cells in the monolayer proliferated to replace released cells (regeneration).

Table 1. [^{3}H]-thymidine incorporation in Madin-Darby canine kidney (MDCK) cells, 24 and 48 hours postincubation with 146 µg calcium oxalate monohydrate crystals

Cell line		24 hours	48 hours
MDCK-I	Control	16.6 ± 0.96	9.06 ± 0.88
	Calcium oxalate monohydrate	15.7 ± 1.36	8.83 ± 2.62
MDCK-II	Control	5.13 ± 0.27	3.95 ± 0.23
	Calcium oxalate monohydrate	5.63 ± 0.21	4.97* ± 0.55

Results expressed as 10^3 dpm/filter insert, ($N = 3$). The incorporation of thymidine was increased in MDCK-II, but not in MDCK-I cells. One day postincubation the *P* value of the unpaired Student *t* test was not yet <0.05 ($P = 0.067$), while 2 days postincubation* the incorporation of [^{3}H]-thymidine in calcium oxalate monohydrate–treated MDCK-II cells was significantly higher compared to untreated controls ($P = 0.041$).

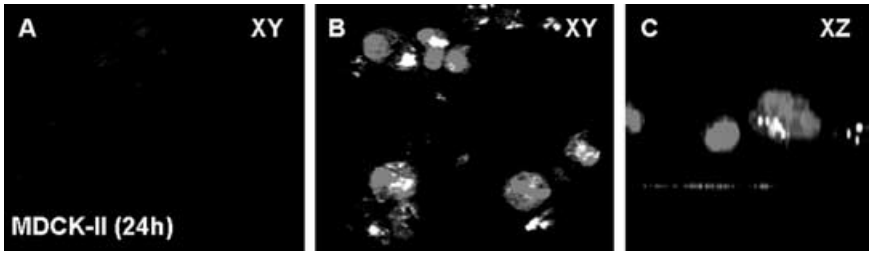

Fig. 7. Crystal-induced pathologic cell death. Confluent monolayers of Madin-Darby canine kidney (MDCK)-II cells are incubated for 24 hours with 146 μg calcium oxalate monohydrate after which the influx of propidium iodide (red) in living cells is studied by CLSM. Crystals are visualized by light reflection (white). There is no influx of propidium iodide in controls (*A*). One day after the addition of crystals, crystal-containing necrotic cells are seen all over the cultures (*B*). An image made perpendicular to the growth substrate revealed that most of the released crystal-containing cells are necrotic (*C*).

Crystal-induced apoptotic or necrotic cell death

To assess if the released crystal-containing cells during the early response are viable or not, these cells were studied for various forms of cell death. Studies were performed in all cell lines. LLC-PK_1 cells were not suitable because there were relatively many necrotic cells in untreated confluent monolayers. The results obtained with $RCCD_1$ were comparable to those obtained with MDCK-I. Confluent monolayers of both MDCK strains were exposed for 24 hours to calcium oxalate monohydrate crystals and then incubated with propidium iodide to find out if crystals are capable to induce pathologic cell death (necrosis). Earlier, we have demonstrated that crystals bind directly to the plasma membranes of MDCK-II and LLC-PK_1 cells, while crystals did not bind to confluent MDCK-I and $RCCD_1$ cells and some force prevented crystals from directly contacting the plasma membrane of proliferating MDCK-I cells. This force appeared to be the invisible pericellular matrix surrounding mobile cells [11]. Our present study shows few necrotic cells in untreated confluent MDCK-II cultures (Fig. 7A). The addition of calcium oxalate monohydrate crystals, however, within 24 hours induced massive cell necrosis as indicated by the ability of propidium iodide to enter nonfixed cells (Fig. 7B). The crystal-containing exfoliated cells from Figure 1 appeared to be necrotic cells (Fig.7C). Figure 8 shows that pathologic cell death only occurs in MDCK-II cells that bind and internalize crystals (Fig. 8F), but not in nonadherent MDCK-I cells (Fig. 8B and D). In addition, this figure shows that 7 days after calcium oxalate monohydrate addition, crystals are still present in the MDCK-II cultures, but do no longer cause necrosis (Fig. 8H).

To reveal if crystals can induce programmed cell death (apoptosis), cells were incubated for 24 hours with calcium oxalate monohydrate after which they were stained with Hoechst 33258 to visualize the DNA. Untreated controls had few apoptotic cells (Fig. 9A). Whereas treatment with the apoptosis-inducer antimycin resulted in DNA fragmentation (Fig. 9C), calcium oxalate monohydrate crystals did not (Fig. 9B). Apoptosis was also studied with annexin V that specifically binds to phophatidylserine at the surface of apoptotic cells. Annexin V bound only minimally to untreated confluent MDCK-I and MDCK-II monolayers (Fig. 10A and D). While treatment with antimycin A resulted in enhanced levels of annexin V binding (Fig. 10C and G), 24 hours with calcium oxalate monohydrate did not increase annexin V binding in either cell type (Fig. 10B and E). Crystals were clearly present in MDCK-II (reflection signals in red in Fig. 10E) and absent in MDCK-I (no reflection signals in the laser light in Fig. 10B), reinforcing the findings in figure 6 and in previously published results [7, 12] that, in contrast to confluent MDCK-II, confluent MDCK-I monolayers do not bind or take up crystals (Fig. 10E).

DISCUSSION

This study shows that calcium oxalate monohydrate crystals are toxic to renal proximal tubular cells, but not to renal collecting tubular cells. Crystals rapidly bind to and are taken up by renal proximal tubular cells, where they induce inflammation (PGE_2), oxidative cell stress (H_2O_2), DNA synthesis ([^{3}H]-thymidine), and pathologic cell death (necrosis). The response to crystals was less marked and without necrotic cell death in renal collecting tubule cells. Two weeks after their initial contact, significant amounts of crystals were still found inside proximal tubular cells, indicating that these cells do not easily remove crystals. Proximal tubular cells showed a biphasic response to crystals. Within 24 hours, approximately half of the cell-associated crystals were released back into the apical fluid compartment (early response), while another 2 weeks were required for the cells to remove again half of the internalized crystals (late response). In contrast to the late response, the early response was accompanied by inflammation-mediated cell death, suggesting that after surviving crystal internalization, the cells accepted the presence of crystals in their interior. Crystals induced increased levels of H_2O_2 in proximal tubular cells as well as in scrape-damaged monolayers, indicating that any form of tissue damage may lead to H_2O_2 generation. Although crystals also slightly increased the production of H_2O_2 in MDCK-I,

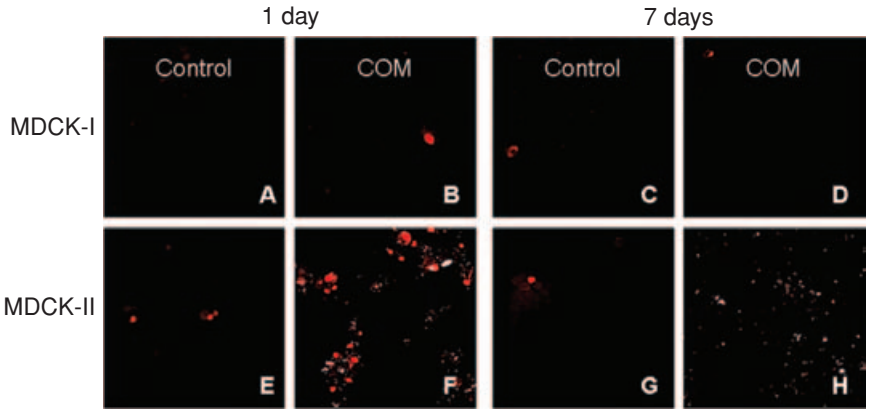

Fig. 8. Influx of propidium iodide (red) in Madin-Darby canine kidney (MDCK) cells in confluent monolayers, 1 and 7 days after calcium oxalate monohydrate (COM) (light reflection, white) addition. Influx only occasionally occurs in control MDCK-I cells (*A* and *C*) and is not increased by calcium oxalate monohydrate (*B* and *D*). Influx seldom occurs in control MDCK-II cells (*E* and *G*). One day after the addition of calcium oxalate monohydrate, crystals became associated with MDCK-II cells (*F*), causing necrosis (F). Seven days later calcium oxalate monohydrate was still present in MDCK-II, but did no longer cause cell necrosis (*H*).

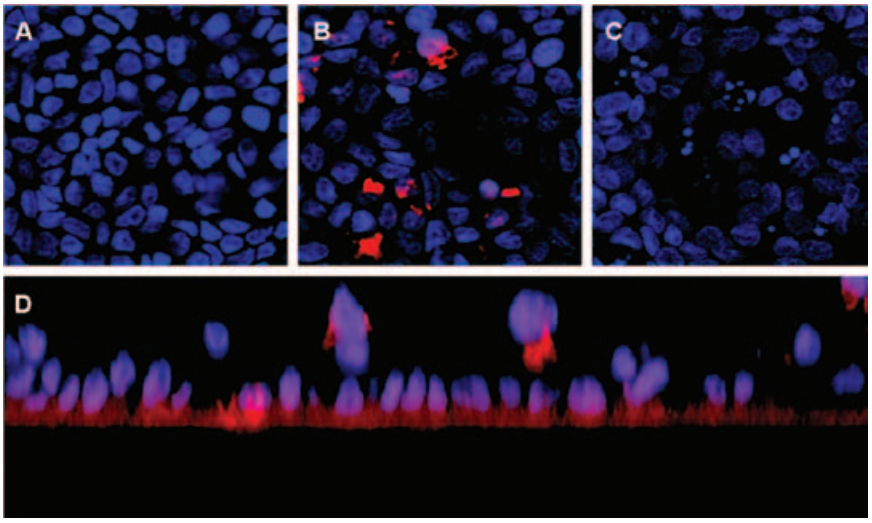

Fig. 9. Hoechst staining (blue) of confluent Madin-Darby canine kidney (MDCK)-II cell monolayers 24 hours after the addition of calcium oxalate monohydrate (COM) crystals (light reflection, red). DNA is not fragmented in untreated controls (*A*) or in cells that received calcim oxalate monohydrate crystals (*B*), while DNA fragmentation is clearly observed in MDCK-II cells treated with antimycin A (*C*). A confocal laser scanning microscopy XZ image made perpendicular to the growth substrate showing that exfoliated crystal–containing cells are not apoptotic.

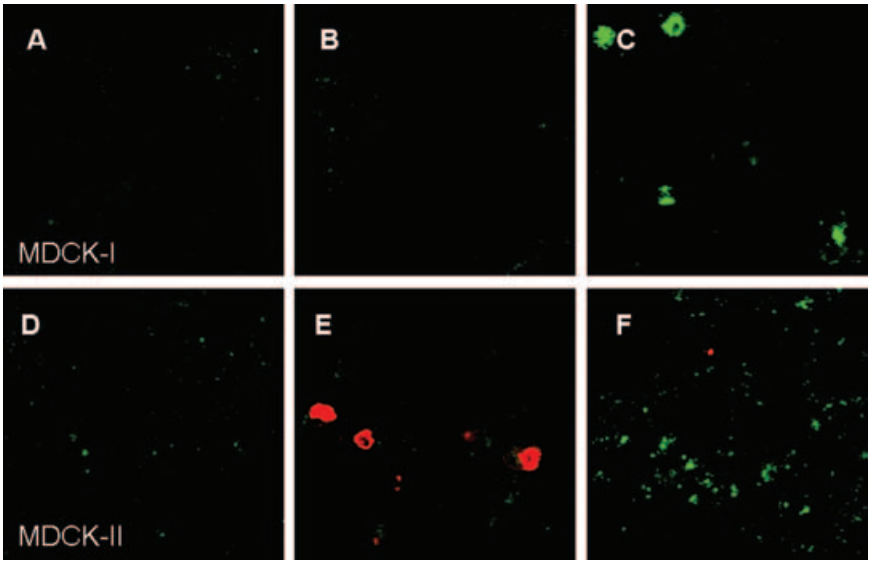

Fig. 10. Confocal laser scanning microscopy of annexin V exhibits minimal binding to confluent monolayers of Madin-Darby canine kidney (MDCK) cells (*A* and *D*). The ability of annexin V to bind to MDCK-I and MDCK-II is increased after pretreatment with antimycin A (*C* and *F*). Calcium oxalate monohydrate crystals do not increase annexin V binding to MDCK-I or MDCK-II cells (*B* and *E*). Propidium iodide influx occurs only in MDCK-II cells incubated with crystals (E).

it should be noted that these cells were nonphysiologically covered for 24 hours with a relatively large amount of crystals that resulted in some cellular response due to suffocation.

Finally, annexin V binding, DNA fragmentation and propidium iodide influx studies clearly demonstrated that crystals induce necrotic cell death without apoptosis.

The concept that crystals induce tissue damage was initially reported in nonrenal tissues such as joints [13], soft tissues [14], cysts of the oral cavity [15], synovial fibroblasts [16], and endothelial cells [17]. Since kidney stones are largely composed of crystals this concept was also introduced in urolithiasis research. Evidence came from rats fed a crystal-inducing diet and from studies performed in cell culture. In 1992, Lieske, Walsh-Reitz, and Toback [18] reported that the internalization of calcium oxalate monohydrate crystals by African green monkey (BSC-1) and MDCK cells stimulated DNA synthesis. Hackett, Shevock, and Khan [19] subsequently found that crystal-containing MDCK and LLC-PK_1 cells were rapidly released from the cultures, which was confirmed in other studies [4, 18, 20–25]. Koul et al [1, 26] found that calcium oxalate monohydrate activates p38 mitogen-activated protein kinase (MAPK) in LLC-PK_1. Crystals increased the mitochondrial production of reactive oxygen species in LLC-PK_1 and MDCK cells with a subsequent depletion of the antioxidant status. The damaging effect of crystals to MDCK cells was inhibited by antioxidants [27]. The concept was born that not only oxalate, but also calcium oxalate crystals cause oxidative stress in renal tubular cells. Although these data collectively support the concept that crystal-cell interaction is damaging to renal tubular cells there is concern about the validity of this hypothesis and the model systems used. Animals, usually rats, are made hyperoxaluric with ammonium oxalate, sodium oxalate, hydroxyproline, or ethylene glycol. Animals treated with these agents excrete higher levels of renal tubular enzymes and histologic examination shows the deposition of crystals at sites where the renal tubules are clearly damaged [28–33]. Recently, our group found that oxalate itself most likely is not nephrotoxic [paper submitted], suggesting that calcium oxalate crystals cause renal tissue damage in rats but the question is how. Based on the results in the present paper and on data in the literature, it is conceivable that an oxalate overload immediately leads to the precipitation of crystals in ultrafiltrate or that somewhere in the nephron tubules are obstructed by large crystal aggregates. It is less likely, however, that subtle crystal-cell interactions trigger inflammatory responses in late segments of the nephron.

In cell culture, damaging effects of crystals were found in MDCK [19, 27, 34–36], LLC-PK_1 [20, 26, 27, 35, 37], opossum kidney-1 (OK-1) [24], BSC-1 [21, 38–40], and NRK52E cells [41–43]. MDCK was established in 1958 from the whole kidney of a dog. The heterogeneous nature of this cell line became clear by the isolation of various strains with completely different properties [5, 44–46]. The LLC-PK_1 and OK-1 cells are widely used as model for the renal proximal tubule and BSC-1 and NRK52E cannot be assigned to a particular segment of the nephron. Thus, although crystal formation occurs in later parts of the nephron, such as the collecting ducts, crystal-cell interaction studies are performed with proximal tubular cells, mixed cell types, or undefined cell types, but not with collecting tubule cells. Data in the literature combined with the results presented in this paper suggest that crystals induce inflammation in cells that are not used to encounter crystals, such as fibroblast [16], endothelial cells [17] and renal proximal tubular cells (this study), but that they do not harm cell types that are frequently confronted with crystals in their environment, like renal collecting duct cells (this study) and most likely the urothelial cells in the remaining urinary tract. To avoid misunderstanding it should be emphasized that this does not include crystals-induced obstruction in the nephron or urinary tract.

The limitations of this study are that we used cell lines derived from different species and it is questionable if they are representative for the human kidney. In addition, these cell types may have lost important functions in cell culture. We cannot exclude the possibility that crystals affect cells in nephron segments that are not included in our set of cell lines. Finally, it is possible that crystals trigger intracellular transduction pathways that were not monitored in our study.

Taken together, our results show that calcium oxalate crystals induce an inflammatory reaction in proximal tubular cells, but not in collecting tubular cells. Crystals bind and enter proximal tubular cells provoking an inflammatory response leading to the exfoliation of necrotic crystal-containing cells that are replaced by new cells. This early reaction is followed by a much milder response during which nonnecrotic crystal-containing cells are gradually eliminated from the monolayer. Crystals did not induce inflammation or necrosis in collecting tubule cells and it is unlikely that they are damaging to the epithelium in the late nephron.

ACKNOWLEDGMENTS

This study was supported by the Dutch Kidney Foundation through grant C98.1780 and by the Oxalosis and Hyperoxaluria Foundation (OHF) through grant 2749036. We thank Professor Marc E de Broe, Dr. Anja Verhulst, and Dr. Benjamin Vervaet of the Department of Nephrology-Hypertension, University of Antwerp, Antwerp, Belgium for valuable discussions.

Reprint requests to Dr. Carl F. Verkoelen, Department of Urology, Sector Kidney Stones Erasmus MC, Rotterdam, The Netherlands; Josephine Nefkens Institute, Room BE330, PO Box 1738, 3000 DR, Rotterdam, The Netherlands.
E-mail: c.verkoelen@erasmusmc.nl

REFERENCES

1. Koul HK: Role of p38 MAP kinase signal transduction in apoptosis and survival of renal epithelial cells. *Ann NY Acad Sci* 1010:62–65, 2003
2. Khan SR, Thamilselvan S: Nephrolithiasis: A consequence of renal epithelial cell exposure to oxalate and calcium oxalate crystals. *Mol Urol* 4:305–312, 2000
3. Scheid CR, Koul H, Hill WA, *et al*: Oxalate ion and calcium oxalate crystal interactions with renal epithelial cells, in *Kidney Stones: Medical and Surgical Management*, edited byCoe FL, Favus MJ, Pak CYC., Parks JH, Preminger GM, Philadelphia, Lippincott-Raven Publishers, 1996, pp 129–143
4. Khan SR: Calcium oxalate crystal interaction with renal tubular epithelium, mechanism of crystal adhesion and its impact on stone development. *Urol Res* 23:71–79, 1995
5. Hansson GC, Simons K, van Meer G: Two strains of the Madin-Darby canine kidney (MDCK) cell line have distinct glycosphingolipid compositions. *Embo J* 5:483–489, 1986
6. Blot-Chabaud M, Laplace M, Cluzeaud F, *et al*: Characteristics of a rat cortical collecting duct cell line that maintains high transepithelial resistance. *Kidney Int* 50:367–376, 1996
7. Schepers MS, Duim RA, Asselman M, *et al*: Internalization of calcium oxalate crystals by renal tubular cells: A nephron segment-specific process? *Kidney Int* 64:493–500, 2003
8. Verkoelen CF, van der Boom BG, Houtsmuller AB, *et al*: Increased calcium oxalate monohydrate crystal binding to injured renal tubular epithelial cells in culture. *Am J Physiol* 274:F958–F965, 1998
9. Verkoelen CF, Romijn JC, de Bruijn WC, *et al*: Association of calcium oxalate monohydrate crystals with MDCK cells. *Kidney Int* 48:129–138, 1995
10. Lifschitz MD: LLC-PK1 Cells derived from pig kidneys have a defect in cyclooxygenase. *J Biol Chem* 257:12611–12615, 1982
11. Schepers MS, Asselman M, Duim RA, *et al*: Pericellular matrix formation by renal tubule epithelial cells in relation to crystal binding. *Nephron Exp Nephrol* 94:E103–E112, 2003
12. Verkoelen CF, van der Boom BG, Kok DJ, *et al*: Cell type-specific acquired protection from crystal adherence by renal tubule cells in culture. *Kidney Int* 55:1426–1433, 1999
13. Denko CW, Whitehouse MW: Experimental inflammation induced by naturally occurring microcrystalline calcium salts. *J Rheumatol* 3:54–62, 1976
14. Denko CW, Petricevic M: Sympathetic or reflex footpad swelling due to crystal-induced inflammation in the opposite foot. *Inflammation* 3:81–86, 1978
15. Aldred MJ, Sugar AW: Calcium oxalate crystals in a nasolabial cyst. *J Oral Maxillofac Surg* 44:149–152, 1986
16. Hasselbacher P: Stimulation of synovial fibroblasts by calcium oxalate and monosodium urate monohydrate. A mechanism of connective tissue degradation in oxalosis and gout. *J Lab Clin Med* 100:977–985, 1982
17. Falasca GF, Ramachandrula A, Kelley KA, *et al*: Superoxide anion production and phagocytosis of crystals by cultured endothelial cells. *Arthritis Rheum* 36:105–116, 1993
18. Lieske JC, Walsh-Reitz MM, Toback FG: Calcium oxalate monohydrate crystals are endocytosed by renal epithelial cells and induce proliferation. *Am J Physiol* 262:F622–F630, 1992
19. Hackett RL, Shevock PN, Khan SR: Madin-Darby canine kidney cells are injured by exposure to oxalate and to calcium oxalate crystals. *Urol Res* 22:197–203, 1994
20. Hackett RL, Shevock PN, Khan SR: Alterations in MDCK and LLC-PK1 cells exposed to oxalate and calcium oxalate monohydrate crystals. *Scanning Microsc* 9:587–596, 1995
21. Lieske JC, Toback FG: Interaction of urinary crystals with renal epithelial cells in the pathogenesis of nephrolithiasis. *Semin Nephrol* 16:458–473, 1996
22. Kohjimoto Y, Ebisuno S, Tamura M, Ohkawa T: Interactions between calcium oxalate monohydrate crystals and Madin-Darby canine kidney cells: Endocytosis and cell proliferation. *Urol Res* 24:193–199, 1996
23. Kohjimoto Y, Ebisuno S, Tamura M, Ohkawa T: Adhesion and endocytosis of calcium oxalate crystals on renal tubular cells. *Scanning Microsc* 10:459–468, 1996
24. Goswami A, Singhal PC, Wagner JD, *et al*: Matrix modulates uptake of calcium oxalate crystals and cell growth of renal epithelial cells. *J Urol* 153:206–211, 1995
25. Ebisuno S, Kohjimoto Y, Tamura M, *et al*: Histological observations of the adhesion and endocytosis of calcium oxalate crystals in MDCK cells and in rat and human kidney. *Urol Int* 58:227–231, 1997
26. Koul HK, Menon M, Chaturvedi LS, *et al*: COM crystals activate the p38 mitogen-activated protein kinase signal transduction pathway in renal epithelial cells. *J Biol Chem* 277:36845–36852, 2002
27. Khand FD, Gordge MP, Robertson WG, *et al*: Mitochondrial superoxide production during oxalate-mediated oxidative stress in renal epithelial cells. *Free Radic Biol Med* 32:1339–1350, 2002
28. Selvam R, Bijikurien T: Effect of citrate feeding on free radical induced changes in experimental urolithiasis. *Indian J Exp Biol* 30:705–710, 1992
29. Khan SR: Animal model of calcium oxalate nephrolithiasis, in *Calcium Oxalate in Biological Systems*, edited byKhan SR, Boca Raton, FL, CRC Press, 1995, pp 343–359
30. de Bruijn WC, Boeve ER, van Run PR, *et al*: Etiology of experimental calcium oxalate monohydrate nephrolithiasis in rats. *Scanning Microsc* 8:541–549, 1994
31. Asselman M, Verhulst A, De Broe ME, Verkoelen CF: Calcium oxalate crystal adherence to hyaluronan-, osteopontin-, and CD44-expressing injured/regenerating tubular epithelial cells in rat kidneys. *J Am Soc Nephrol* 14:3155–3166, 2003
32. Khan SR, Shevock PN, Hackett RL: Acute hyperoxaluria, renal injury and calcium oxalate urolithiasis. *J Urol* 147:226–230, 1992
33. Khan SR, Shevock PN, Hackett RL: Urinary enzymes and calcium oxalate urolithiasis. *J Urol* 142:846–849, 1989
34. Thamilselvan S, Khan SR: Oxalate and calcium oxalate crystals are injurious to renal epithelial cells: results of in vivo and in vitro studies. *J Nephrol* 11 (Suppl 1):66–69, 1998
35. Khan SR, Byer KJ, Thamilselvan S, *et al*: Crystal-cell interaction and apoptosis in oxalate-associated injury of renal epithelial cells. *J Am Soc Nephrol* 10 (Suppl 14):S457–S463, 1999
36. Kohjimoto Y, Kennington L, Scheid CR, Honeyman TW: Role of phospholipase A_2 in the cytotoxic effects of oxalate in cultured renal epithelial cells. *Kidney Int* 56:1432–1441, 1999
37. Thamilselvan S, Khan SR, Menon M: Oxalate and calcium oxalate mediated free radical toxicity in renal epithelial cells: Effect of antioxidants. *Urol Res* 31:3–9, 2003
38. Lieske JC, Spargo BH, Toback FG: Endocytosis of calcium oxalate crystals and proliferation of renal tubular epithelial cells in a patient with type 1 primary hyperoxaluria. *J Urol* 148:1517–1519, 1992
39. Lieske JC, Swift H, Martin T, *et al*: Renal epithelial cells rapidly bind and internalize calcium oxalate monohydrate crystals. *Proc Natl Acad Sci USA* 91:6987–6991, 1994
40. Lieske JC, Toback FG: Regulation of renal epithelial cell endocytosis of calcium oxalate monohydrate crystals. *Am J Physiol* 264:F800–F807, 1993
41. Umekawa T, Chegini N, Khan SR: Oxalate ions and calcium oxalate crystals stimulate MCP-1 expression by renal epithelial cells. *Kidney Int* 61:105–112, 2002
42. Umekawa T, Chegini N, Khan SR: Increased expression of monocyte chemoattractant protein-1 (MCP-1) by renal epithelial cells in culture on exposure to calcium oxalate, phosphate and uric acid crystals. *Nephrol Dial Transplant* 18:664–669, 2003
43. Miller C, Kennington L, Cooney R, *et al*: Oxalate toxicity in renal epithelial cells: Characteristics of apoptosis and necrosis. *Toxicol Appl Pharmacol* 162:132–141, 2000
44. Balcarova-Stander J, Pfeiffer SE, Fuller SD, Simons K: Development of cell surface polarity in the epithelial Madin-Darby canine kidney (MDCK) cell line. *Embo J* 3:2687–2694, 1984
45. Valentich JD: Morphological similarities between the dog kidney cell line MDCK and the mammalian cortical collecting tubule. *Ann NY Acad Sci* 372:384–405, 1981
46. Gekle M, Wunsch S, Oberleithner H, Silbernagl S: Characterization of two MDCK-cell subtypes as a model system to study principal cell and intercalated cell properties. *Pflugers Arch* 428:157–162, 1994